Journal of Cellular Biochemistry 104:51–58 (2008)

Confocal Fluorescence Microscopy Study of Interaction Between Lens MIP26/AQP0 and Crystallins in Living Cells

Bing-Fen Liu and Jack J Liang*

Ophthalmic Research/Surgery, Brigham and Women's Hospital; Department of Ophthalmology, Harvard Medical School, Boston, Massachusetts 02115

Abstract MIP26/AQP0 is the major lens fiber membrane protein and has been reported to interact with many other lens components including crystallins, lipid, and cytoskeletal proteins. Regarding crystallins, many previous reports indicate that MIP26/AQP0 interacts with either only α-crystallin or some specific γ-crystallins. Considering the possibly important role of MIP26/AQP0 in the reduction of light scattering in the lenses, we have further investigated its interaction with crystallins using confocal fluorescence resonance energy transfer (FRET) microscopy. Specifically, we used MIP26 tagged with a green fluorescence protein (GFP) as a donor and a crystallin (αA-, αB-, βB2-, or γC-crystallin) tagged with a red fluorescence protein (RFP) as an acceptor. The two plasmids were cotransfected to HeLa cells. After culture, laser scattering microscopy images were taken in each of the three channels: GFP, RFP, and FRET. The net FRET images were then obtained by removing the contribution of spectral bleed-through. The pixels of net FRET were normalized with those of GFP. The results show the presence of measurable interactions between MIP26 and all crystallins, with the extent of interactions decreasing from αA- and αB-crystallin to βB2- and γC-crystallin. Competitive interaction study using untagged αA-crystallin shows decreased net FRET, indicating specificity of the interactions between MIP26 and αA-crystallin. We conclude that all crystallins interact with MIP26, the physiological significance of which may be a reduction in the difference of refractive index between membrane and cytoplasm. J. Cell. Biochem. 104: 51–58, 2008.

Key words: aquaporin 0; FRET; confocal FRET microscopy; crystalline; GFP; MIP26

MIP26, also known as aquaporin 0 (AQP0), is the major protein of the lens fiber cell membrane, where its function has been suggested to be water transport [Varadaraj et al., 1999]. Structural studies indicate that it has six transmembrane domains and intracellularly localized N- and C-termini [Gorin et al., 1984; Reizer et al., 1993]. A mutant MIP26 gene has been shown to be associated with autosomal dominant polymorphic and lamellar cataract [Berry et al., 2000; Francis et al., 2000a], and missense MIP26 genes E134G and T138R mutants have been identified in dominantly inherited cataracts [Francis et al., 2000b]. These studies point to a possible role for MIP26 in lens transparency and cataractogenesis.

Most biological functions require proteins to form complexes. In the lens, various crystallins and other lens cytoplasmic proteins associate to form complexes that serve as refractive index gradients. The short-range order among crystallins in the lens or in a highly concentrated protein solution is an example of one protein interacting with the nearest neighboring proteins [Delaye and Tardieu, 1983]. Other kinds of interactions among crystallins may exist in dilute solutions [Mach et al., 1990; Fu and Liang, 2002; Ponce and Takemoto, 2005]. Interactions between crystallins and cytoskeletal proteins also have been suggested [Gopalakrishnan et al., 1993; Perng et al., 1999; Fujita et al., 2004]. As for interactions between

This article contains supplementary material, which may be viewed at the Journal of Cellular Biochemistry website at http://www.interscience.wiley.com/jpages/0730-2312/suppmat/index.html.

Grant sponsor: National Institutes of Health; Grant number: EY13968; Grant sponsor: Massachusetts Lions Eye Research Fund.

*Correspondence to: Jack J Liang, 221 Longwood Ave, Boston MA 02115. E-mail: jliang@rics.bwh.harvard.edu

Received 20 June 2007; Accepted 7 September 2007

DOI 10.1002/jcb.21598

crystallins and membrane protein, reports are conflicting. Some studies using isolated crystallins and MIP26 suggest binding between MIP26 and α-crystallin [Mulders et al., 1985; Liang and Li, 1992], but other studies assert that α-crystallin binds only to lipids [Ifeanyi and Takemoto, 1989; Cobb and Petrash, 2002a,b]. A recent study of confocal fluorescence microscopy provides evidence that two members of the γ-crystallin family interact with MIP26 [Fan et al., 2005]. Here we seek to confirm and to quantify the interactions between MIP26 and either α-, β-, or γ-crystallin using confocal fluorescence resonance energy transfer (FRET) microscopy.

MATERIALS AND METHODS

Preparation of Expression Constructs

pAcGFP-C1 and pDsRed Monomer-C1 vectors were obtained from Clontech (Palo Alto, CA). MIP26 cDNA in a pYES2 plasmid (a gift from Dr. Peter Agre of Duke University) was subcloned into pAcGFP-C1 vector, and crystallin genes from a previous study (αA, αB, βB2, and γC) [Fu and Liang, 2002] were subcloned to pDsRed Monomer-C1 vector. The pAcGFP-C1 vector was encoded with a green fluorescence protein (GFP, $\lambda_{ex}/\lambda_{em} = 475/505$ nm), and the pDsRed Monomer-C1 vector was encoded with a red fluorescence protein (RFP, $\lambda_{ex}/\lambda_{em} = 557/585$ nm). The PCR used forward primers containing *Xho*I for each crystallin and *EcoR*I for MIP26, and reverse primers containing an *EcoR*I site for each crystallin and *BamH*I for MIP26 (Table I). The resulting constructs were designated GFP-MIP, RFP-αA, RFP-αB, RFP-βB2, and RFP-γC.

For the positive and negative controls, p53, SV40 large tumor antigen (T), and polyoma virus coat protein (CP) were used. It is known that p53 interacts with T and not with CP [Li and Fields, 1993]. Constructs of GFP-p53, RFP-T, and RFP-CP were prepared by subcloning p53 gene to pAcGFP-C1 using *Kpn*I/*BamH*I restriction enzymes, and T or CP gene to pDsRed Monomer-C1 using *Xho*I and *EcoR*I restriction enzymes (Table I).

Cell Culture

HeLa cells were cultured with the protocol described in our recent report [Liu et al., 2007]. Briefly, HeLa cells (1×10^5/ml) were seeded into a 35-mm culture dish and co-transfected with their respective vectors with target inserts using the lipofactamine 2000 reagent at the ratio 1:2 (1.6 μg of each cDNA: 3.2 μg of lipofactamine 2000). For controls, either GFP-MIP26 or RFP-crystallin construct was transfected alone. After incubation for 48 h, living cell images were acquired with a Zeiss Laser Scanning Microscope (LSM) (510 META Axioplan 2, Carl Zeiss, Inc., Thornwood, NY).

In the competitive interaction or inhibitory experiments, an equal amount of the untagged αA-crystallin cDNA was included in cotransfection of GFP-MIP26 and RFP-αA-crystallin.

Confocal FRET Microscopy

Confocal images were acquired with a Zeiss Laser Scanning Microscope (LSM) 510 META Axioplan 2 confocal microscope (Carl Zeiss, Inc.) at the Harvard Center for Neurodegeneration & Repair, Optical Imaging Facility as described previously [Liu et al., 2007]. Briefly, Images (12-bit) of multitrack channels with the following configuration were recorded: an argon/2 laser (25 mW, T1 and T3 = 10% of laser exposure) for the GFP channel (donor excitation/donor

TABLE I. The Forward and Reverse Primers for Subcloning Experiments for Confocal Microscopy

	Forward primers	Reverse primers
GFP-p53[a]	AACAAGCTTCACAGGACCCTGTCACCGAGACC	A GAA TTCTCAGTCTGAGTCAGGCCC
RFP-T[b]	CTTCTCGAGCTGGAACTGATGAA TGGGAGC	GGGGAATTCAGTTTGGACAAACCAC
RFP-CP[b]	GTTCTCGACTGCG TTGATACCA TGG	GGAA TTCTTAGAGACG CCG CTT
GFP-MIP[c]	TCGAATTCGTGGGAACTGCGATCAGC	TTTGGATCCCTACAGGGCCTGGGT
RFP-αA[c]	GACCCTCGAGCTGACGTGACCATCCAG	AGCCTAGAATTCTTAGGACGAGGGAGC
RFP-αB[b]	AACCCTCGAGCTGACATCGCCATCCAC	CAGGAGGAATTCCTATTTCTTGGGGGC
RFP-βB2[b]	GAACCTCGAGCTGCCTCAGATCACCAG	GGTCTAGAATTCCTAGTTGGAGGGGTG
RFP-γC[b]	TAGCCTCGAGCTGGGAAGATCACCTTC	CGCCGCGAATTCTTAATACAAATCCAC

[a]The underlined sequences are for *Hind*III and *EcoR*I restriction sites for 5′ and 3′ primers, respectively.
[b]The underlined sequences are for *xho*I and *EcoR*I restriction sites for 5′ and 3′ primers, respectively.
[c]The underlined sequences are for *EcoR*I and *BamH*I restriction sites for 5′ and 3′ primers, respectively.

emission: $GFP_{ex/em}$) and FRET channel (donor excitation/acceptor emission: $FRET_{ex/em}$) with excitation wavelength at 488 nm, and a HeNe 1 Laser (T2 = 100%) for the RFP channel (acceptor excitation/acceptor emission: $RFP_{ex/em}$) with excitation wavelength at 543 nm. The images were obtained by adjusting the parameters of the instrument (pinhole, detection gain etc.) to avoid saturation of the images and the imaging parameters were kept constant throughout the experiments. Three sets of cell specimens were included in imaging: cells transfected with donor only, cells transfected with acceptor only, and cells cotransfected with both donor and acceptor. In each set of experiment, typically 50–100 region of interest (ROI) were chosen from many cell images.

The LSM images were analyzed as described before [Liu et al., 2007]. Briefly, the intensities of total gray values in the three channels, I_{GFP} ($\lambda_{ex}/\lambda_{em} = 475/505$ nm), I_{RFP} (557/585 nm), and I_{FRET} (475/585 nm) were measured in the same ROI. After adjustment of threshold, the net FRET (I_{nFRET}) values were obtained by correcting contribution from spectral bleed-through (SBT) of the donor and acceptor in the FRET channel with the equation [Xia and Liu, 2001]:

$$I_{nFRET} = I_{FRET} - (I_{RFP} \times a) - (I_{GFP} \times b) \quad (1)$$

where a is the coefficient due to SBT of an acceptor signal to the FRET channel and b is the coefficient due to SBT of a donor signal to the FRET channel. SBT arises from overlapping of spectra: donor SBT from overlapping of part of the emission spectrum of the donor with emission spectrum of the acceptor, and acceptor SBT from overlapping of part of the excitation spectrum of the acceptor with excitation spectrum of the donor (shaded areas in the supplemental figure). The two coefficients were determined with cells expressing RFP-crystallin construct alone (with RED signal but no GFP signal) or GFP-MIP26 construct alone (with GFP signal but no RED signal), and were defined by the following equations:

$$a = I_{FRETex/em}/I_{RFPex/em} \quad (2)$$

and

$$b = I_{FRETex/em}/I_{GFPex/em} \quad (3)$$

The calculated I_{nFRET} values were normalized with I_{GFP} intensity to make them comparable among different ROIs and cells.

Statistical Analysis

Data are expressed as the mean ± SE from a minimum of three independent experiments. Statistical analysis was performed with student's *t*-test using Sigmaplot statistical analysis software, with $P < 0.05$ as the criterion of significance.

RESULTS

Initial experiments with positive and negative controls indicated that fluorescence intensity in the FRET channel was significantly higher in cells expressing positive control p53-T than in cells expressing negative control p53-CP (Fig. 1). The nFRET images were also converted to pseudo-color for assessing the range of pixel values. In the calculation of net FRET, the SBT coefficients a and b were obtained from cells expressing RFP-T (RFP-CP) or GFP-p53 alone. The two coefficients a and b were used in calculation of net FRET according to Equation (1). Finally the normalized I_{nFRET}/I_{GFP} values were obtained. I_{nFRET}/I_{GFP} values are significantly larger for p53-T than for p53-CP (Fig. 2). The results demonstrate the feasibility of the technique for detecting protein–protein interactions by energy transfer between two fused proteins.

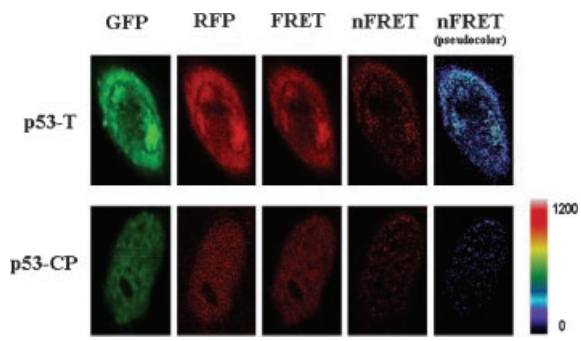

Fig. 1. Representative confocal LSM images of cells cotransfected with positive (p53-T) and negative (p53-CP) controls. GFP-p53 and SV40 large tumor antigen (RFP-T) or GFP-p53 and polyoma virus coat protein (RFP-CP) were cotransfected to HeLa cells. After culture, LSM images of living cells were taken from each of the three channels with the following excitation and emission wavelengths: GFP (475/505 nm), RFP (557/585 nm), and FRET (475/585 nm). Shown on the top of the columns are the labels for the images from the three channels (GFP, RFP, and FRET) as well as nFRET images (red and pseudo-color). Shown on the **left panel** are the labels for the positive control GFP(p53)-RFP(T) and negative control GFP(p53)-RFP(CP). The color bar represents the relative degree of net FRET shown in the pseudocolor images.

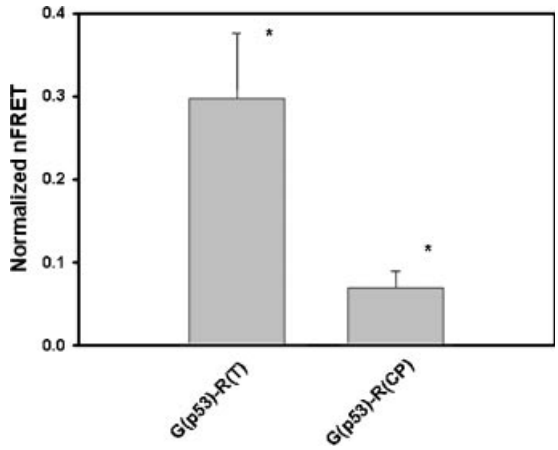

Fig. 2. Normalized nFRET of the positive control p53-T and negative control p53-CP. The normalized nFRET values were obtained by normalizing I_{nFRET} with I_{GFP}. The nFRET values are the average of region of interest (ROI's) (n = 40) in three transfection experiments. There was significant difference between positive and negative control (*$P < 0.001$).

LSM images from the three channels GFP, RFP, and FRET as well as nFRET for MIP26-crystallin are shown in Figure 3. MIP26 was localized mostly around the plasma and nuclear membrane regions with little cytoplasmic expression, and some large aggregates were detected. A similar expression pattern has been reported previously [Fan et al., 2005]. As for crystallins, while αA- and αB-crystallins are mostly distributed in cytoplasm, βB2-and γC-crystallins can be seen throughout the whole cells. Therefore, ROIs were chosen along the membrane region.

From ROIs of the nFRET images, the parameters I_{GFP}, I_{RFP}, I_{FRET}, I_{nFRET}, and I_{nFRET}/I_{GFP} were calculated. The normalized I_{nFRET}/I_{GFP} values were plotted in Figure 4, which indicated that MIP26 interacted with all crystallins but to a significantly different extent; αA-crystallin showed the highest interaction with MIP26.

Competitive interaction experiments using the untagged αA-crystallin cDNA in the cotransfection showed a decrease in nFRET between GFP-MIP26 and RFP-αA, indicating that the available donor (GFP-MIP26) was competitively removed by untagged αA-crystallin. The data are included in Figure 4. The results of competitive binding indicated that the FRET value became very small relative to the control p53-CP, but the difference is still statistically significant ($P < 0.001$).

DISCUSSION

Our recent study of protein–protein interactions of lens crystallins using tagged GFP and RFP by confocal FRET provides a good example of the technique's versatility [Liu et al., 2007]. In FRET, the energy is nonradiatively transferred from the donor protein to the acceptor protein when they are expressed in very close proximity (20–50 Å) and when donor emission spectrum overlaps with acceptor absorption spectrum [Wu and Brand, 1994; Liang and Liu, 2006]. The other factor of relative orientation of the donor and acceptor transition dipoles was usually considered constant and not dealt with much in the literature. The major problem in FRET confocal microscopy is the spectral bleed-through that gives unwanted signal in the FRET channel, resulting in a higher observed FRET signal than the actual signal. We used an approach that removed this contribution with the control experiments and correction analysis defined by Equations (1–3) [Xia and Liu, 2001]. The results of negative control (p53-CP) indicate that some negligible signal cannot be removed and may be treated as background signal.

Our experimental design is intended to confirm the interaction between MIP26 and crystallins. Previous reports have indicated that interaction sites with crystallins can be either lipids or MIP26, and both have been demonstrated to interact with α-crystallin [Mulders et al., 1985; Ifeanyi and Takemoto, 1989; Liang and Li, 1992; Cobb and Petrash, 2002a]. Membrane lipids are amphipathic molecules with hydrophilic or polar head groups and hydrophobic tails. Most phospholipids are bilayer structures, in which the polar phosphorylated groups are located on the surfaces and the hydrophobic fatty chains are buried in the core. The binding between the outer polar groups and crystallins most likely involves charge–charge interactions. Therefore, it is not surprising that only α-crystallin interacts with membrane lipids [Ifeanyi and Takemoto, 1989; Cobb and Petrash, 2002a], as α-crystallin has a greater charge than β- and γ-crystallins under physiological conditions. Since previous reports have shown interaction between MIP26 and α-crystallin and some γ-crystallins, we feel it important to extend this investigation.

Protein–protein interactions are dictated by many factors, such as hydrophobicity, solvent

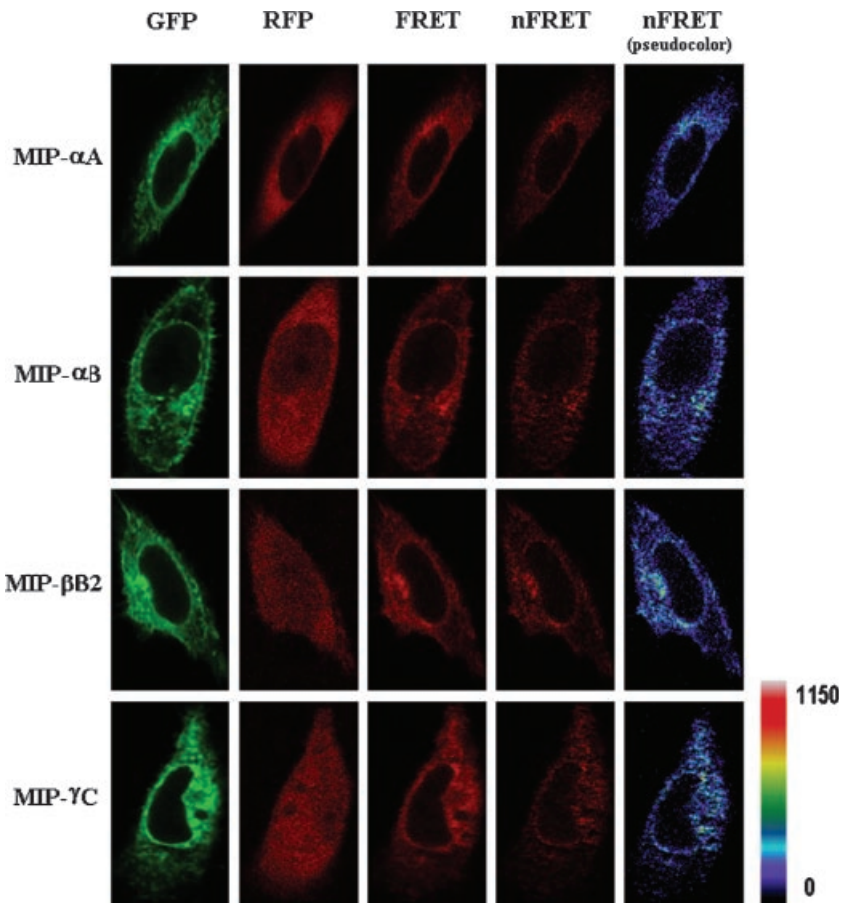

Fig. 3. Representative confocal LSM images of cells cotransfected with MIP26 and various crystallins. GFP-MIP26 and each RFP-crystallin were cotransfected to HeLa cells. After culture, LSM images of living cells were taken from each of the three channels with the following excitation and emission wavelengths: GFP (475/505 nm), RFP (557/585 nm), and FRET (475/585 nm). Shown on the top of the columns are the labels for the images from the three channels (GFP, RFP, and FRET) as well as nFRET images (red and pseudo-color). Shown on the **left panel** are the labels for the pairs of GFP(MIP)-RFP(crystallin). The color bar represents relative degree of net FRET shown in the pseudocolor images.

accessibility, and residue pairing preferences, which in turn are determined by the amino acid sequence and protein structural aspects. The β-sheet domain comprising many β-strands has been suggested as one of the sites of protein–protein interactions [Hoskins et al., 2006]. There are plenty of β-strands in crystallins, containing 30–60% β-sheet conformation based on CD study [Liang and Chakrabarti, 1982; Liang et al., 1985]. CD and FTIR spectroscopic studies also show that MIP26/AQP0 contains a high amount (30–40%) of β-sheet [Van Hoek et al., 1993]. The β-sheet domain interaction is partially responsible for the intra- and intermolecular domain association in lens crystallins

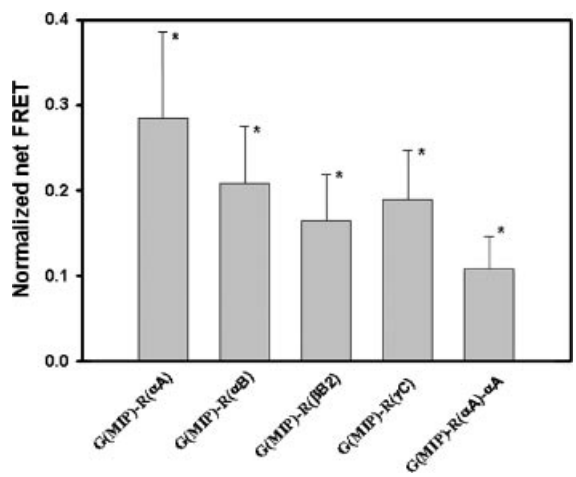

Fig. 4. Normalized nFRET of MIP26 coexpressed with various crystallins. The nFRET values are the average of region of interest (ROI's) (n = 50–90) in 3–4 transfection experiments. The last bar is the result of inhibitory experiments in cotransfection with additional untagged αA-crystallin cDNA. Significant differences were observed (*$P < 0.001$ compared with all pairs). The results from inhibitory experiments are also included, in which an equal amount of untagged αA-crystallin was cotransfected with GFP-MIP26 and RFP-αA.

[White et al., 1989; Koteiche and McHaourab, 1999; Ghosh and Clark, 2005; Liu and Liang, 2006]. In addition to the β-sheet domain interaction, a hydrophobic interaction may also be involved, based on observations that αA- and αB-crystallin have greater hydrophobicity [Liang et al., 2000] and thus greater interactions with MIP26 than βB2- and γC-crystallin.

Recently, confocal fluorescence microscopy studies of interactions between rodent lens MIP26 and γ-crystallins were reported [Fan et al., 2004, 2005]. These studies used mammalian RK13 cells co-transfected with EGFP-tagged MIP expression plasmid and HcRED-tagged γ-crystallin expression plasmid. Spatial quantification along a path across the plasma membrane was performed; evidence for co-localization included the finding that both EGFP and HcRed fluorescence peaked at the vicinity of the plasma membrane. The results suggest that γE- and γF-crystallins, but not other γ-crystallins (γA, γB-, γC- γD-, and γS-), were recruited to the membrane by interaction with MIP26. However, co-localization of two proteins may not be definite proof of direct interactions. Confocal FRET microscopy provides more convincing evidence. It is possible that the conflicting results between the previous report and ours on the interaction between MIP26 and γC-crystallin are due to different methodology in detection. Furthermore, the functional significance of interaction between MIP26 and γE/γF-crystallin diminishes, because the CRYGE and CRYGF genes in human are non-functional pseudogenes [Brakenhoff et al., 1990; Heon et al., 1999].

MIP26 is the lens-specific membrane protein; expression in HeLa cells may be somewhat different from that in the lens fiber cells. The majority of expression was in plasma and nuclear membrane regions, though there was minor cytoplasmic expression. There were some protein aggregates in which strong fluorescence of both donor and acceptor were seen. A similar expression pattern has been reported in mammalian RK13 cells [Fan et al., 2005]. In calculation of the net FRET, we always chose the ROI in the membrane regions where strong fluorescence signals were observed. One may argue whether the use of HeLa cells in the present study is appropriate, but considering that the cells were merely used as hosting media for detection of protein interaction and not for studying protein or cell function, the choice of hosting cells should not be important.

The function of the lens is to focus the image on the retina, which is achieved by refraction at interfaces due to difference in refractive indices [Bettelheim, 2004]. Although refractive index in the membrane is higher than in the cytoplasm, the difference decreases from cortex to nucleus [Michael et al., 2003]. The difference in refractive index between the membrane and cytoplasm gives rise to light scattering in the lens, but association between membrane and crystallins may decrease the refractive index difference. Therefore, the amount of light scattering in the normal lens is very small. The greater light scattering in aged and cataractous lenses is due to a large fluctuation in refractive index from structural changes [Bettelheim, 2004].

A possible interacting site for MIP26 is the cytoplasmic C-terminal segment (amino acid sequence from 225 to 263), which has been reported to be biologically active; it is the interaction site with some cytoskeletal proteins and gap junction proteins [Yu et al., 2005; Lindsey Rose et al., 2006]. The C-terminal segment also is susceptible to post-translational modifications including phosphorylation, deamidation, and truncation; processes that increase with age [Takemoto and Takehana, 1986; Schey et al., 2000; Ball et al., 2004]. Since cleavage in the C-terminal region increases in the nucleus, the interaction between MIP26 and crystallins should decrease. The decreased interaction will have minimal effect on lens biology because there is little difference in refractive index between membrane and cytoplasm in the lens nucleus [Michael et al., 2003].

In conclusion, our results demonstrate that MIP26/AQP0 interacts with the four major crystallins (αA-, αB-, βB2-, and γC-crystallins) and an appreciable increase of interaction is observed with αA- and αB-crystallins. Our findings confirm previous reports of association of MIP26 with crystallins [Mulders et al., 1985; Liang and Li, 1992; Fan et al., 2005]. The biological significance of the association is reduction of differences of refractive index in the interfaces of membrane and cytoplasm.

ACKNOWLEDGMENTS

The authors are grateful to Dr. Peter Agre of Duke University for providing human MIP26/

AQP0 clone. Technical assistance from Mark Hanson is gratefully acknowledged.

REFERENCES

Ball LE, Garland DL, Crouch RK, Schey KL. 2004. Post-translational modifications of aquaporin 0 (AQP0) in the normal human lens: Spatial and temporal occurrence. Biochemistry 43:9856–9865.

Berry V, Francis P, Kaushal S, Moore A, Bhattacharya S. 2000. Missense mutations in MIP underlie autosomal dominant 'polymorphic' and lamellar cataracts linked to 12q. Nat Genet 25:15–17.

Bettelheim FA. 2004. Light scattering in lens research: An essay on accomplishments and promises. Exp Eye Res 79:747–752.

Brakenhoff RH, Aarts HJ, Reek FH, Lubsen NH, Schoenmakers JG. 1990. Human gamma-crystallin genes. A gene family on its way to extinction. J Mol Biol 216:519–532.

Cobb BA, Petrash JM. 2002a. alpha-crystallin chaperone-like activity and membrane binding in age-related cataracts. Biochemistry 41:483–490.

Cobb BA, Petrash JM. 2002b. Factors influencing alpha-crystallin association with phospholipid vesicles. Mol Vis 8:85–93.

Delaye M, Tardieu A. 1983. Short-range order of crystallin proteins accounts for eye lens transparency. Nature 302: 415–417.

Fan J, Donovan AK, Ledee DR, Zelenka PS, Fariss RN, Chepelinsky AB. 2004. gammaE-crystallin recruitment to the plasma membrane by specific interaction between lens MIP/aquaporin-0 and gammaE-crystallin. Invest Ophthalmol Vis Sci 45:863–871.

Fan J, Fariss RN, Purkiss AG, Slingsby C, Sandilands A, Quinlan R, Wistow G, Chepelinsky AB. 2005. Specific interaction between lens MIP/Aquaporin-0 and two members of the gamma-crystallin family. Mol Vis 11: 76–87.

Francis P, Berry V, Bhattacharya S, Moore A. 2000a. Congenital progressive polymorphic cataract caused by a mutation in the major intrinsic protein of the lens, MIP (AQP0). Br J Ophthalmol 84:1376–1379.

Francis P, Chung JJ, Yasui M, Berry V, Moore A, Wyatt MK, Wistow G, Bhattacharya SS, Agre P. 2000b. Functional impairment of lens aquaporin in two families with dominantly inherited cataracts. Hum Mol Genet 9:2329–2334.

Fu L, Liang JJ. 2002. Detection of protein-protein interactions among lens crystallins in a mammalian two-hybrid system assay. J Biol Chem 277:4255–4260.

Fujita Y, Ohto E, Katayama E, Atomi Y. 2004. alphaB-crystallin-coated MAP microtubule resists nocodazole and calcium-induced disassembly. J Cell Sci 117:1719–1726.

Ghosh JG, Clark JI. 2005. Insights into the domains required for dimerization and assembly of human alphaB crystallin. Protein Sci 14:684–695.

Gopalakrishnan S, Boyle D, Takemoto L. 1993. Association of actin with alpha crystallins. Trans Kans Acad Sci 96:7–12.

Gorin MB, Yancey SB, Cline J, Revel JP, Horwitz J. 1984. The major intrinsic protein (MIP) of the bovine lens fiber membrane: Characterization and structure based on cDNA cloning. Cell 39:49–59.

Heon E, Priston M, Schorderet DF, Billingsley GD, Girard PO, Lubsen N, Munier FL. 1999. The gamma-crystallins and human cataracts: A puzzle made clearer. Am J Hum Genet 65:1261–1267.

Hoskins J, Lovell S, Blundell TL. 2006. An algorithm for predicting protein-protein interaction sites: Abnormally exposed amino acid residues and secondary structure elements. Protein Sci 15:1017–1029.

Ifeanyi F, Takemoto L. 1989. Differential binding of alpha-crystallins to bovine lens membrane. Exp Eye Res 49: 143–147.

Koteiche HA, McHaourab HS. 1999. Folding pattern of the alpha-crystallin domain in alphaA-crystallin determined by site-directed spin labeling. J Mol Biol 294:561–577.

Li B, Fields S. 1993. Identification of mutations in p53 that affect its binding to SV40 large T antigen by using the yeast two-hybrid system. FASEB J 7:957–963.

Liang JN, Chakrabarti B. 1982. Spectroscopic investigations of bovine lens crystallins. 1. Circular dichroism and intrinsic fluorescence. Biochemistry 21:1847–1852.

Liang JJ, Li XY. 1992. Spectroscopic studies on the interaction of calf lens membranes with crystallins. Exp Eye Res 54:719–724.

Liang JJ, Liu BF. 2006. Fluorescence resonance energy transfer study of subunit exchange in human lens crystallins and congenital cataract crystallin mutants. Protein Sci 15:1619–1627.

Liang JN, Andley UP, Chylack LT, Jr. 1985. Spectroscopic studies on human lens crystallins. Biochim Biophys Acta 832:197–203.

Liang JJ, Sun TX, Akhtar NJ. 2000. Heat-induced conformational change of human lens recombinant alphaA- and alphaB-crystallins. Mol Vis 6:10–14.

Lindsey Rose KM, Gourdie RG, Prescott AR, Quinlan RA, Crouch RK, Schey KL. 2006. The C terminus of lens aquaporin 0 interacts with the cytoskeletal proteins filensin and CP49. Invest Ophthalmol Vis Sci 47:1562–1570.

Liu BF, Liang JJ. 2006. Domain interaction sites of human lens betaB2-crystallin. J Biol Chem 281:2624–2630.

Liu BF, Anbarasu K, Liang JJ. 2007. Confocal fluorescence resonance energy transfer microscopy study of protein-protein interactions of lens crystallins in living cells. Mol Vis 13:854–861.

Mach H, Trautman PA, Thomson JA, Lewis RV, Middaugh CR. 1990. Inhibition of alpha-crystallin aggregation by gamma-crystallin. J Biol Chem 265:4844–4848.

Michael R, van Marle J, Vrensen GF, van den Berg TJ. 2003. Changes in the refractive index of lens fibre membranes during maturation—Impact on lens transparency. Exp Eye Res 77:93–99.

Mulders JW, Stokkermans J, Leunissen JA, Benedetti EL, Bloemendal H, de Jong WW. 1985. Interaction of alpha-crystallin with lens plasma membranes. Affinity for MP26. Eur J Biochem 152:721–728.

Perng MD, Cairns L, van den IP, Prescott A, Hutcheson AM, Quinlan RA. 1999. Intermediate filament interactions can be altered by HSP27 and alphaB-crystallin. J Cell Sci 112:2099–2112.

Ponce A, Takemoto L. 2005. Screening of crystallin-crystallin interactions using microequilibrium dialysis. Mol Vis 11:752–757.

Reizer J, Reizer A, Saier MH, Jr. 1993. The MIP family of integral membrane channel proteins: Sequence comparisons, evolutionary relationships, reconstructed pathway of evolution, and proposed functional differentiation of the two repeated halves of the proteins. Crit Rev Biochem Mol Biol 28:235–257.

Schey KL, Little M, Fowler JG, Crouch RK. 2000. Characterization of human lens major intrinsic protein structure. Invest Ophthalmol Vis Sci 41:175–182.

Takemoto L, Takehana M. 1986. Major intrinsic polypeptide (MIP26K) from human lens membrane: Characterization of low-molecular-weight forms in the aging human lens. Exp Eye Res 43:661–667.

Van Hoek AN, Wiener M, Bicknese S, Miercke L, Biwersi J, Verkman AS. 1993. Secondary structure analysis of purified functional CHIP28 water channels by CD and FTIR spectroscopy. Biochemistry 32:11847–11856.

Varadaraj K, Kushmerick C, Baldo GJ, Bassnett S, Shiels A, Mathias RT. 1999. The role of MIP in lens fiber cell membrane transport. J Membr Biol 170:191–203.

White HE, Driessen HP, Slingsby C, Moss DS, Lindley PF. 1989. Packing interactions in the eye-lens. Structural analysis, internal symmetry and lattice interactions of bovine gamma IVa-crystallin. J Mol Biol 207:217–235.

Wu P, Brand L. 1994. Resonance energy transfer: Methods and applications. Anal Biochem 218:1–13.

Xia Z, Liu Y. 2001. Reliable and global measurement of fluorescence resonance energy transfer using fluorescence microscopes. Biophys J 81:2395–2402.

Yu XS, Yin X, Lafer EM, Jiang JX. 2005. Developmental regulation of the direct interaction between the intracellular loop of connexin 45.6 and the C terminus of major intrinsic protein (aquaporin-0). J Biol Chem 280:22081–22090.